

^{64}Cu levels from the $^{62}\text{Ni}(^3\text{He},p)$ reaction at 18 MeV

A. K. Basak

*Department of Physics, Rajshahi University, Rajshahi, Bangladesh
and International Centre for Theoretical Physics, Trieste, Italy*

M. A. Basher, A. S. Mondal, M. A. Uddin, S. Bhattacharjee, and A. Husain

Department of Physics, Rajshahi University, Rajshahi, Bangladesh

S. K. Das and Masudul Haque

Department of Physics, Shahjalal University of Science and Technology, Sylhet, Bangladesh

H. M. Sen Gupta

Department of Physics, Dhaka University, Dhaka, Bangladesh

(Received 13 January 1997)

The $(^3\text{He},p)$ reaction has been studied on ^{62}Ni using a beam of 18 MeV ^3He particles. Angular distributions of the outgoing protons have been measured for 65 levels including the new levels at 2.323, 3.231, 5.043, and 7.339 MeV and the analog states at 6.821 MeV ($0^+;4$) and 8.188 MeV ($2^+;4$) in the angular range $\theta_{\text{lab}}=5^\circ-80^\circ$. Data have been analyzed in terms of the distorted-wave Born approximation (DWBA). The L transfers have been obtained, J^π limits have been assigned, and the normalization constant has been deduced for several low-lying states. [S0556-2813(97)03709-6]

PACS number(s): 25.55.Hp, 27.50.+e

I. INTRODUCTION

The $(^3\text{He},p)$ reaction is used to study the wave functions and spectroscopy of the final nuclear states and is expected to excite preferentially states with dominant np -pair correlations. The differential cross sections of the reaction are therefore strongly dependent on the wave functions involved.

The ^{64}Cu levels have been investigated using various reactions [1-15]. Park and Daehnick [3] used the (d,a) reaction to study ^{64}Cu up to $E_x=2.9$ MeV. The $(^3\text{He},p)$ or (a,d) reaction is a useful supplement in the study of the level scheme of ^{64}Cu . The (a,d) reactions, because of their relatively high reaction Q values, favor larger angular momentum transfers compared to those in the $(^3\text{He},p)$ reaction.

The present work on the $^{62}\text{Ni}(^3\text{He},p)$ reaction was undertaken for two reasons. First the levels of ^{64}Cu have not been studied using the $(^3\text{He},p)$ reaction, except for the only other measurement by Young and Rapaport [15] at 13 MeV, but no details are given. The second purpose was to examine how well the shell model calculations in the model space of $2p_{3/2}$, $1f_{5/2}$, and $2p_{1/2}$ orbits outside the ^{56}Ni core work for at least the low-lying positive parity states of ^{64}Cu . This is because the two-nucleon transfer reactions are highly sensitive to the details of the wave functions, as many different configurations of the transferred nucleon pair can contribute to the process.

II. EXPERIMENTAL PROCEDURE

The experiment was carried out with a beam of 18 MeV ^3He particles from the Tandem Van de Graaff of AERE, Harwell. The target was self-supporting, isotopically enriched to 99% ^{62}Ni and of thickness $100 \mu\text{g cm}^{-2}$. It was placed at the center of a multichannel magnetic spectrograph.

The reaction products were magnetically analyzed under a field strength of 12.45 kG and recorded in Ilford L4 nuclear emulsion plates of thickness $25 \mu\text{m}$ simultaneously over the angles $5^\circ-80^\circ$ (lab) in a step of 7.5° . The plates were cov-

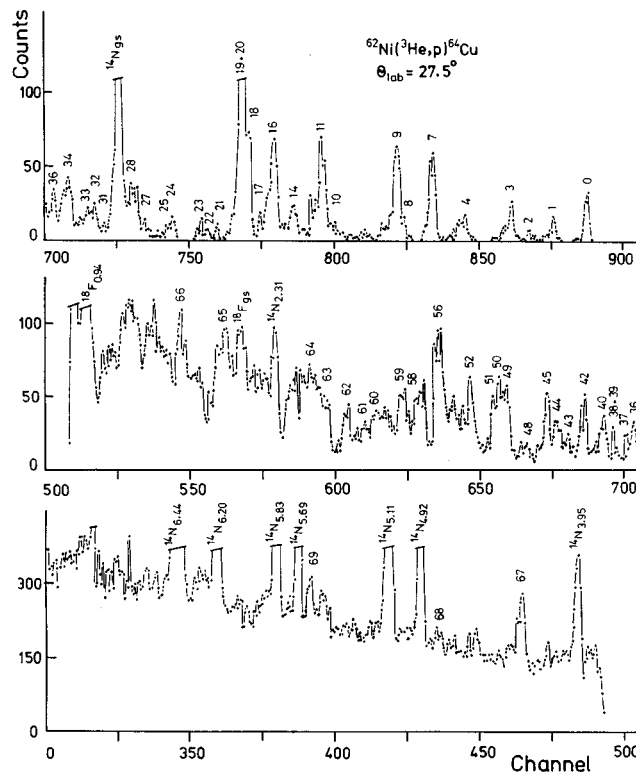


FIG. 1. Proton spectrum at 27.5° arising from the $^{62}\text{Ni}(^3\text{He},p)^{64}\text{Cu}$ reaction.

TABLE I. The optical model parameters (lengths in fm and depths in MeV). $V' = 54.145 - 0.22E$, $V_1 = 58.127 - 0.32E$, $V_2 = 58.731 - 0.55E$, $V_3 = 65.43 - 0.30E$, $W_{3d} = 10.54 - 0.06E$, $W' = 1.2 + 0.09E$, $W_1 = 0.22E - 2.7$ or 0 , $r' = 1.15 - 0.001E$, $W'_d = 4.962 - 0.05E$, $W_{1d} = 12.39 - 0.25E$, $a_w = 0.789 - 0.008E$.

	${}^3\text{He}$	${}^3\text{He}$	${}^3\text{He}$	p	p	p	p	n,p	n,p
Set	<i>H1</i>	<i>H2</i>	<i>H3</i>	<i>P1</i>	<i>P2</i>	<i>P3</i>	<i>P4</i>	<i>B1</i>	<i>B2</i>
V	93.86	157.1	178.7	V'	V_1	V_2	V_3	^a	^a
r_0	1.15	1.20	1.113	1.16	1.17	1.25	r'	1.17	1.25
a	0.75	0.708	0.774	0.75	0.75	0.65	0.57	0.70	0.65
W				W'	W_1		W_3		
$4W_D$	96.36	112.0	120.7	$4W'_d$	$4W_{1d}$	54.0	$4W_{3d}$		
r_I	1.35	1.218	1.242	1.37	1.32	1.25	r'		
a_I	0.80	0.836	0.755	a_w	0.544	0.47	0.50		
V_{SO}				6.04	6.20	7.5	5.45	$\lambda = 25$	$\lambda = 25$
r_{SO}				1.064	1.01	1.25	r'	1.17	1.25
a_{SO}				0.78	0.75	0.65	0.57	0.70	0.65
r_0	1.4	1.4	1.4	1.25	1.3	1.25	1.25	1.25	1.25
Ref.	^b	^c	^c	^d	^e	^f	^g		

^aAdjusted for bound state.

^bTrost *et al.* [17].

^cShepard *et al.* [18].

^dMenet *et al.* [19].

^eBecchetti and Greenlees [20].

^fPerey [21].

^gWatson *et al.* [22].

ered with 1 mm thick polythene foil so as to stop all particles less penetrating than protons. The total beam charge was 10,124 μC . Stop factors of 4 and 2 were used for the two most forward angles; namely, 5° and 12.5° , respectively.

The plates were scanned at the University of Rajshahi,

Rajshahi and the energy spectra were obtained at various angles. A typical spectrum at 27.5° (lab) is shown in Fig. 1. The proton groups from the different levels in ${}^{64}\text{Cu}$ for which the angular distributions of cross section have been measured, are labeled. The overall energy resolution [full

TABLE II. Spectroscopic amplitudes for populating the states of the final nucleus.

E_x (MeV)	$(J^\pi; T)$	ΔT	$(f_{5/2})^2$	$f_{5/2} \cdot p_{3/2}$	$f_{5/2} \cdot p_{1/2}$	$(p_{3/2})^2$	$p_{3/2} \cdot p_{1/2}$	$(p_{1/2})^2$
0.0	$(1^+; 3)$	0	^a -0.159	-0.301		-0.050	0.081	-0.023
0.663	$(1^+; 3)$	0	^b -0.234	-0.024		-0.241	-0.210	-0.045
0.927	$(1^+; 3)$	0	^a -0.256	-0.024		-0.264	-0.231	-0.045
0.160	$(2^+; 3)$	0	^a 0.327	0.033	0.341	-0.122	0.195	0.032
0.278	$(2^+; 3)$	0	^b 0.359	0.033	0.002	-0.133	0.214	0.032
0.608	$(2^+; 3)$	0	^a 0.039	-0.525	-0.095	-0.028	0.289	
0.745	$(2^+; 3)$	0	^a -0.216	0.152	-0.080	-0.186	0.476	
0.362	$(2^+; 3)$	0	^a 0.136	-0.095	0.015	-0.502	-0.193	
0.574	$(2^+; 3)$	0	^a -0.095	-0.095	0.269	0.006	0.006	
6.821	$(0^+; 4)$	1	^a -0.193	0.117	-0.317	0.094	0.029	
8.188	$(2^+; 4)$	1	^a 0.092	0.418	0.034			
0.574	$(4^+; 3)$	0	^a	0.411				
6.821	$(0^+; 4)$	1	^a 0.006	-0.626		-0.695		-0.574
8.188	$(2^+; 4)$	1	^a -1.036					
0.362	$(3^+; 3)$	0	^a					
0.574	$(4^+; 3)$	0	^a	0.411				
6.821	$(0^+; 4)$	1	^a 0.006	-0.626				
8.188	$(2^+; 4)$	1	^a -1.036					
0.362	$(3^+; 3)$	0	^a					
0.574	$(4^+; 3)$	0	^a	0.411				
6.821	$(0^+; 4)$	1	^a 0.006	-0.626		-0.695		-0.574
8.188	$(2^+; 4)$	1	^a -1.036					
0.362	$(3^+; 3)$	0	^a					
0.574	$(4^+; 3)$	0	^a	0.411				
6.821	$(0^+; 4)$	1	^a 0.006	-0.626		-0.695		-0.574
8.188	$(2^+; 4)$	1	^a -1.036					
0.362	$(3^+; 3)$	0	^a					
0.574	$(4^+; 3)$	0	^a	0.411				
6.821	$(0^+; 4)$	1	^a 0.006	-0.626		-0.695		-0.574
8.188	$(2^+; 4)$	1	^a -1.036					

^aShell model spectroscopic amplitudes [30].

^bModified set of spectroscopic amplitudes.

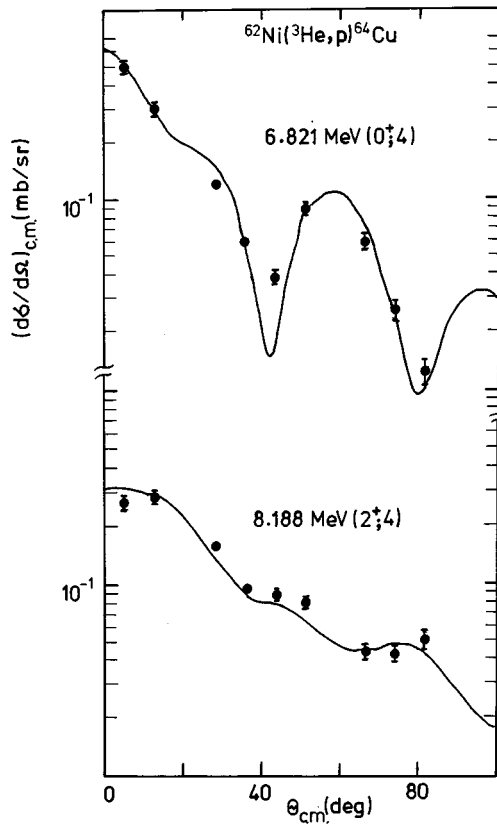


FIG. 2. The measured differential cross sections for the reaction to the analog states at 6.821 and 8.188 MeV excitation. The solid curves are the DWBA predictions using the optical parameter sets $H3$, $P1$, and $B2$, and shell model spectroscopic amplitudes.

width at half maximum (FWHM)] was found to be ≈ 37 keV. A number of levels were observed up to ~ 8.2 MeV excitation with statistical uncertainties less than 10 keV. The energy levels were obtained by a parabolic fit to several well established levels in ^{64}Cu as well as the contaminant levels of ^{14}N and ^{18}F arising, respectively, from ^{12}C and ^{16}O . The criteria used for the identification of levels were that they had about the same width at different angles and that the excitation energies were consistent to within about 10 keV over the angles.

III. DWBA ANALYSIS

The microscopic distorted-wave Born approximation (DWBA) analyses were carried out using the code DWUCK4 of Kunz [16]. The optical model potential was of the standard Woods-Saxon form for the real and volume imaginary parts of the potential, and its derivative form for the surface imaginary and spin-orbit terms. A Coulomb potential due to a uniformly charged spherical nucleus of radius $R_c = r_c A^{1/3}$ was added to the above potential. The optical potential parameter sets for the entrance and the outgoing channels as well as the bound states are given in Table I.

The bound state wave functions for each of the transferred nucleons were generated by assuming a real Woods-Saxon well with the depth adjusted to give each nucleon a separation energy equal to half the separation energy of the ($S=1, T=0$) np pair. The binding energy of the transferred

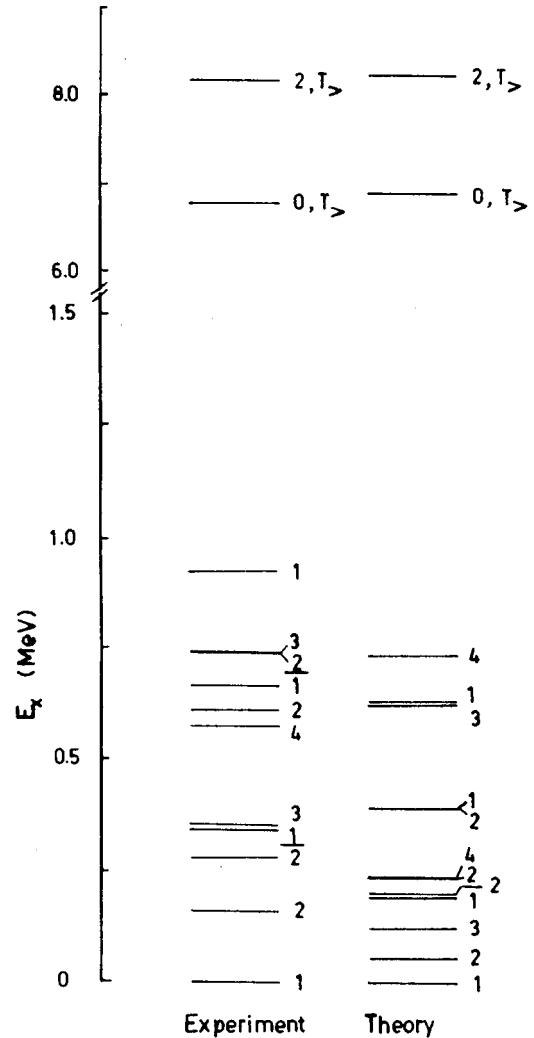


FIG. 3. A comparison between the low-lying positive parity levels including two analog states given from the shell model calculations and as observed [32]. Levels shown underlined are either not observed or weakly populated in the ($^3\text{He},p$) reaction.

pair in the singlet state ($S=0, T=1$) was taken to be deeper by 2.225 MeV. A Thomas-Fermi spin-orbit term [23] with $\lambda=25$ was also used for the bound state wave functions. Corrections due to the nonlocality [24,25] of potential in the conventional form were applied using the nonlocality ranges $\beta(^3\text{He})=0.22$ fm and $\beta_p=0.85$ fm. No finite-range [26] correction was applied to the bound states, as the use of the finite-range parameter greater than 0.5 leads to absurd predictions.

To begin with, detailed DWBA analyses were performed by using the data for the reaction populating the 6.821 MeV ($0^+;4$) analog ground state. This state can be populated by simple configurations, e.g., (i) by the $L=0$ transfer only and (ii) by the spin-isospin ($S=0, T=1$) transfers only. Moreover the shell-model configuration as can be seen in Table II is also simple, both the transferred nucleons being in the same orbits. Of the various potential sets, the combination of $H3$ for the incoming channel, $P1$ for the outgoing channel, and $B2$ for the bound state has produced the best fit to the data, which is shown in Fig. 2.

In the absence of a spin-orbit interaction, the experimental

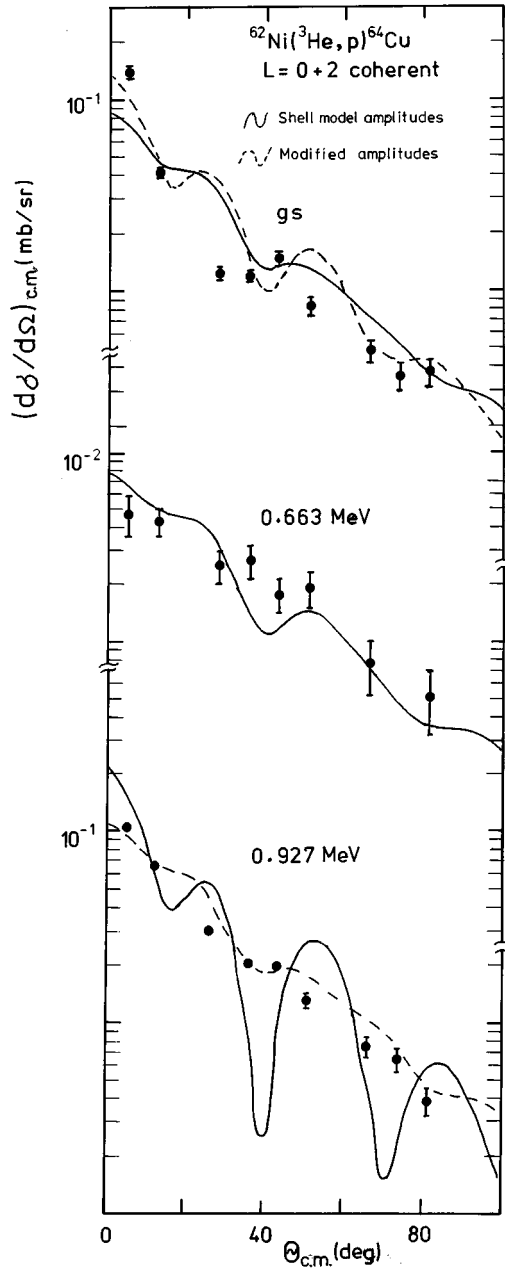


FIG. 4. The measured angular distributions are compared with the DWBA predictions using the coherent contributions from the $L=0$ and 2 transfers and the shell model spectroscopic amplitudes.

cross-section $\sigma_{\text{exp}}(\theta)$ is related to $\sigma_{DW}(ST, \theta)$, the predicted cross section for spin S and isospin T transfers by the DWUCK4 code through the expression [27]

$$\sigma_{\text{exp}}(\theta) = N \frac{2J_f + 1}{2J_i + 1} \sum_{ST} b_{ST}^2 |D_{ST}|^2 (2S + 1) \frac{\sigma_{DW}(ST, \theta)}{2j + 1}, \quad (1)$$

where the light particle spectroscopic amplitude b_{ST} and the mixing factor for the interaction potential D_{ST} have been defined by Towner and Hardy [27,28]. N is the normalization factor for the reaction as defined by Nann *et al.* [29].

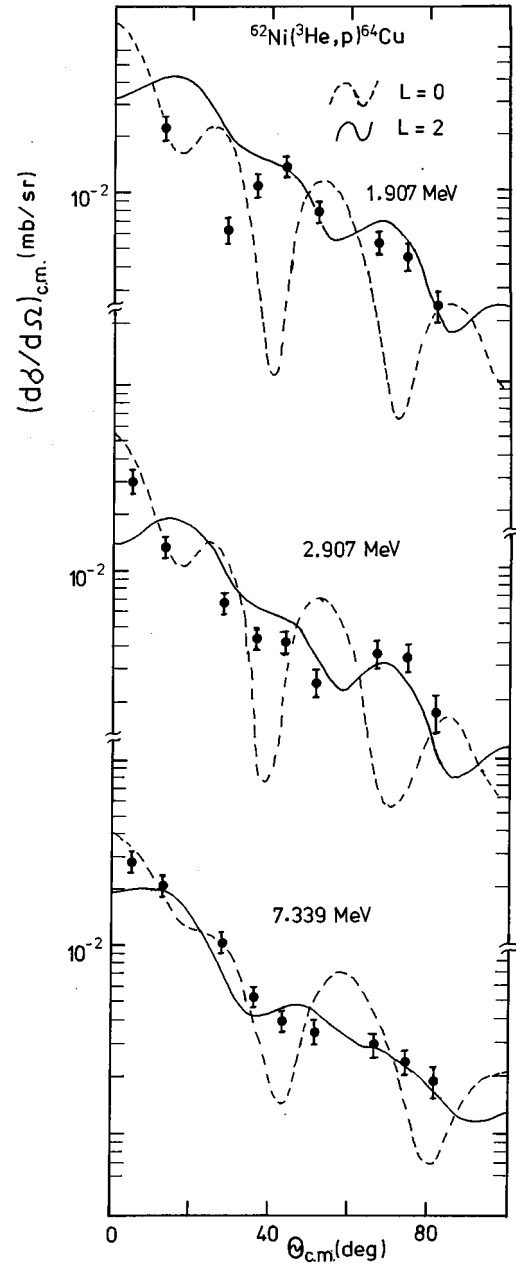


FIG. 5. The measured angular distributions are compared with the DWBA predictions, full curve for $L=2$ and broken curve for $L=0$ transfers.

Using $b_{01}^2 = b_{10}^2 = \frac{1}{2}$ and defining $R = |D_{10}|^2 / |D_{01}|^2$ and $N = N |D_{01}|^2 / 2$, one can write the following relations for the $^{62}\text{Ni}(^3\text{He}, p)$ reaction:

$$(i) \quad \sigma_{\text{exp}}(\theta) = N \sigma_{DW}(01, \theta) \quad (2a)$$

for the analog transitions,

$$(ii) \quad \sigma_{\text{exp}}(\theta) = 3RN \sigma_{DW}(01, \theta) \quad (2b)$$

for the unnatural J transfers and

$$(iii) \quad \sigma_{\text{exp}}(\theta) = N \sigma_{DW}(\theta) \quad (2c)$$

for the natural J transfers with

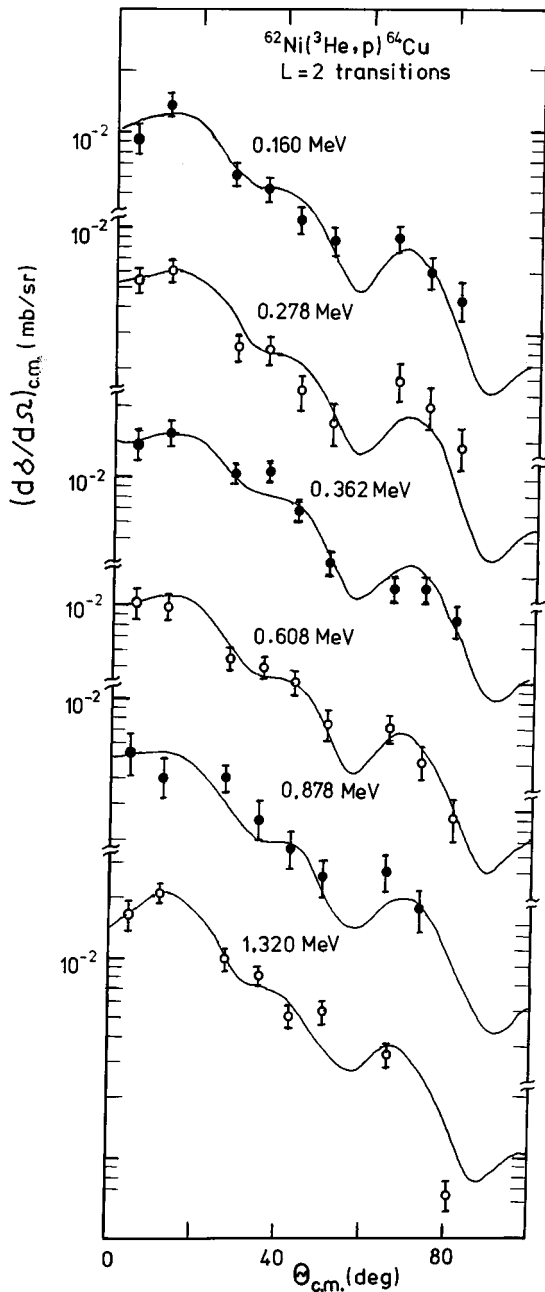


FIG. 6. The measured angular distributions are compared with the $L=2$ DWBA predictions. The predictions for the 0.160, 0.278, 0.362, and 0.608 MeV states are calculated with the spectroscopic amplitudes in Table II.

$$\sigma_{DW}(\theta) = \sigma_{DW}(01, \theta) + 3R\sigma_{DW}(10, \theta).$$

In the present work $R=0.4$ following Hardy and Towner [28] has been used.

IV. RESULTS

Shell model calculations are carried out using the code OXBASH to extract the spectroscopic amplitudes for the microscopic DWBA analysis of the angular distributions to levels in ^{64}Cu having a dominant $(2p_{3/2}, 1f_{5/2}, 2p_{1/2})$ configuration outside the closed ^{56}Ni core [30]. The shell model code uses the two-body matrix elements of Koops and Glau-

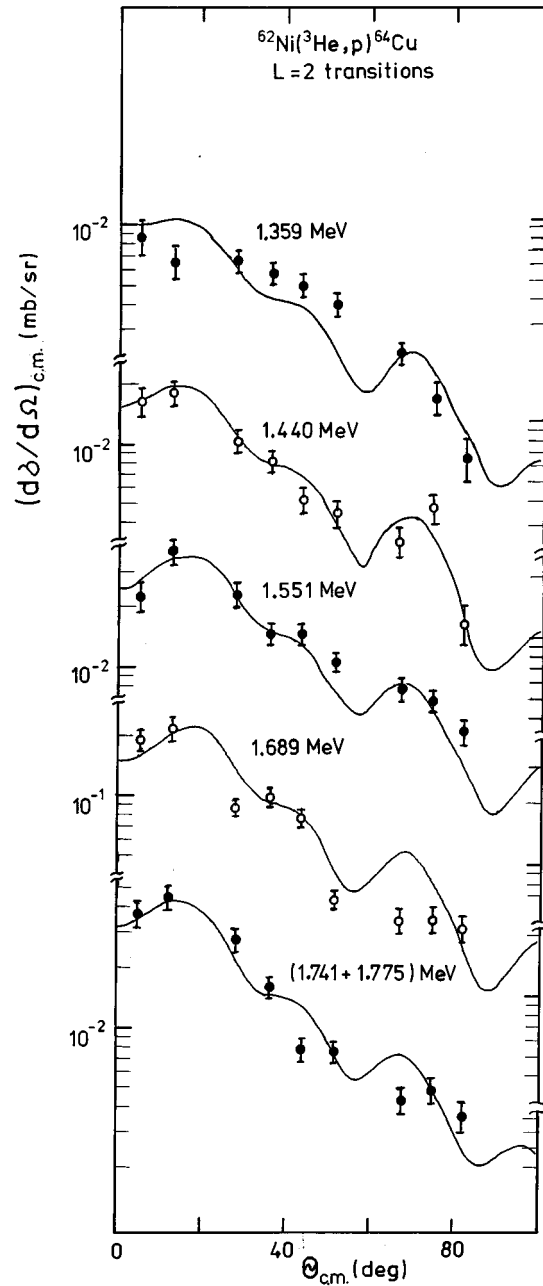


FIG. 7. The measured angular distributions are compared with the $L=2$ DWBA predictions.

demans [31] for the modified surface δ interaction (MSDI).

The low-lying positive parity levels including the analogs of the ground and the first excited states obtained as above are shown in Fig. 3 for a comparison with the known (positive parity) levels in ^{64}Cu (summarized by Singh [32]). Most of the levels are reproduced to better than 150 keV or so. The rather large difference in position between the shell model 4_1^+ level and the observation is disturbing. The 4_2^+ level has not been definitely identified. There are several levels excited in different reactions without a definite J^π assignment. One of these, in particular the one at $E_x \sim 0.663$ MeV as discussed later, may be a good candidate for this shell model level. The levels shown underlined in the figure; namely, $E_x = 0.344$ and 0.739 MeV with $J^\pi = 1^+$ and 2^+ respectively are either not at all populated in the $(^3\text{He}, p)$ reaction (present work)

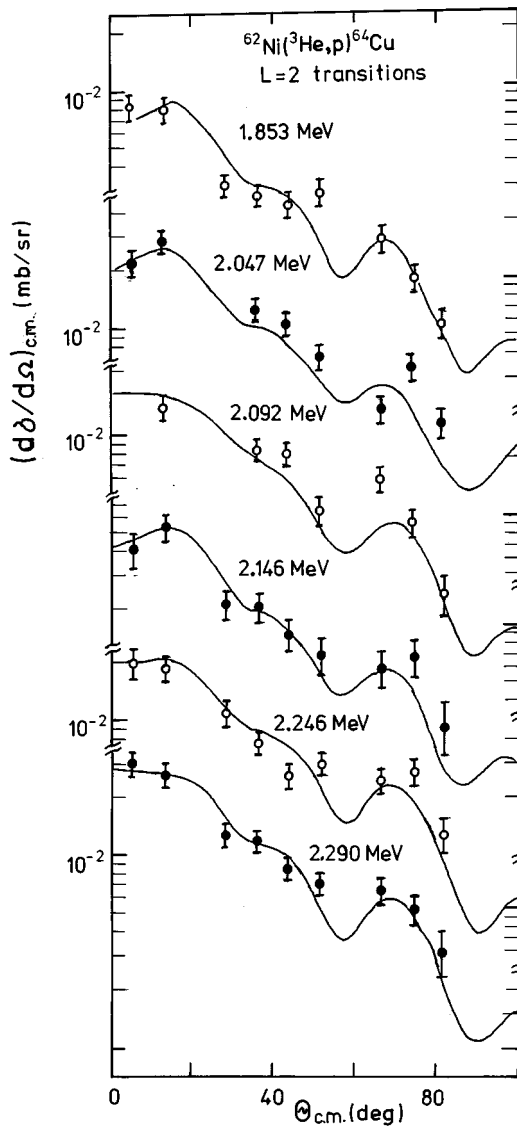


FIG. 8. Same as in Fig. 6.

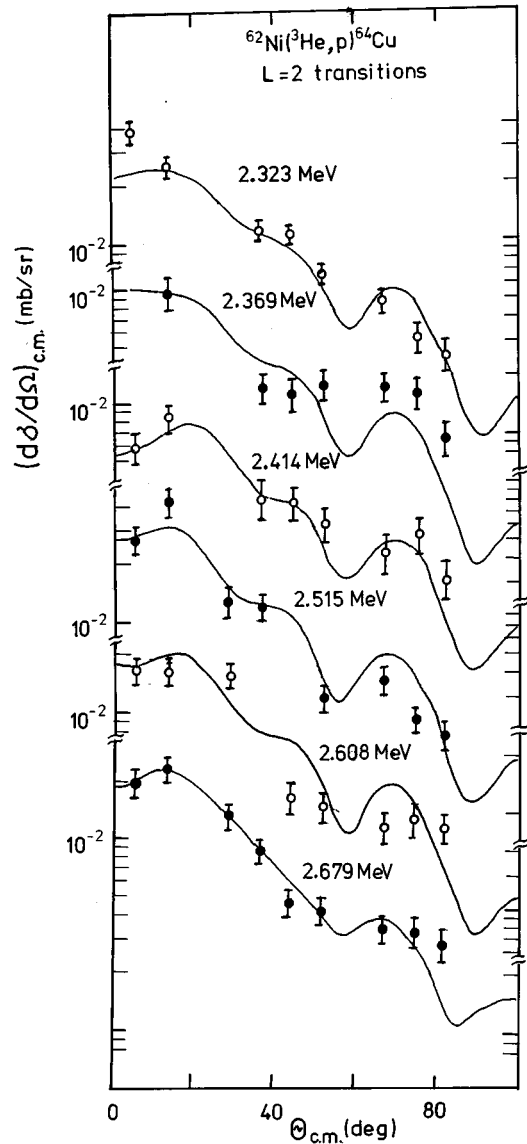


FIG. 9. Same as in Fig. 6.

and (d,a) reaction [3] or very weakly excited.

The spectroscopic amplitudes obtained as above with $2p_{3/2}$, $1f_{5/2}$, and $2p_{1/2}$ active orbits are given in Table II. The DWBA calculations for the transitions to the ground $(1^+;3)$, 0.663 MeV $(1^+;3)$, 0.927 MeV $(1^+;3)$, 0.160 MeV $(2^+;3)$, 0.278 MeV $(2^+;3)$, 0.608 MeV $(2^+;3)$, 0.745 MeV $(2^+;3)$, 0.362 MeV $(3^+;3)$, 0.574 MeV $(4^+;3)$, 6.821 MeV $(0^+;4)$, and 8.188 MeV $(2^+;4)$ states were made using these amplitudes.

The measured and the predicted angular distributions are shown in Figs. 2, 4–17. Error in the absolute cross sections arises mainly from the target thickness. Repeated extraction of the peak area revealed no more than 5% uncertainty from the background subtraction and even less for strong groups and those appearing in the clear regions of the spectrum. The total uncertainty in the absolute cross sections is less than 25%. The predicted cross sections for the ground, 0.663 and 0.927 MeV states with $J^\pi, T = 1^+;3$, have been compared to the data in Fig. 4. The solid curves which are the DWBA predictions with shell model amplitudes in Table II, produce poor fits to the ground state data and even worse fits to the

0.927 MeV data. Better fits have been achieved using empirically modified sets of spectroscopic amplitudes (Table II), where the predictions are shown in broken curves. The angular distributions for the three states need both $L=0$ and 2 transfers.

The angular distributions for the analog states [32] at 6.821 and 8.188 MeV excitations, are well fitted (Fig. 2) by the DWBA calculations using the shell model amplitudes in Table II. The ground state analog is known to be a doublet at $E_x = 6.810$ and 6.826 MeV [32], but these are not resolved in the present work.

The cross section data for the 0.160, 0.278, 0.362, and 0.608 MeV states in Fig. 6 are also reproduced well by the $L=2$ DWBA predictions using the shell model amplitudes in Table II. Figures 6–11 show the angular distributions to other final states, fitted to the $L=2$ DWBA predictions using simple np -orbital configuration. The orbital effects have been found to be small.

The predictions using the shell model spectroscopic amplitudes for the 0.745 MeV $(2^+;3)$ and 0.574 MeV $(4^+;3)$ states have been compared to the angular distribution data in

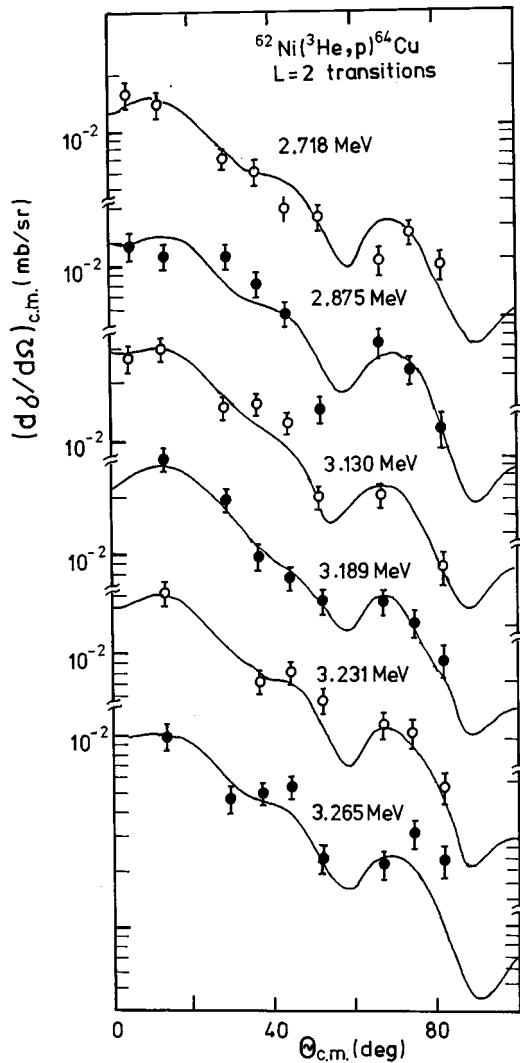


FIG. 10. Same as in Fig. 6.

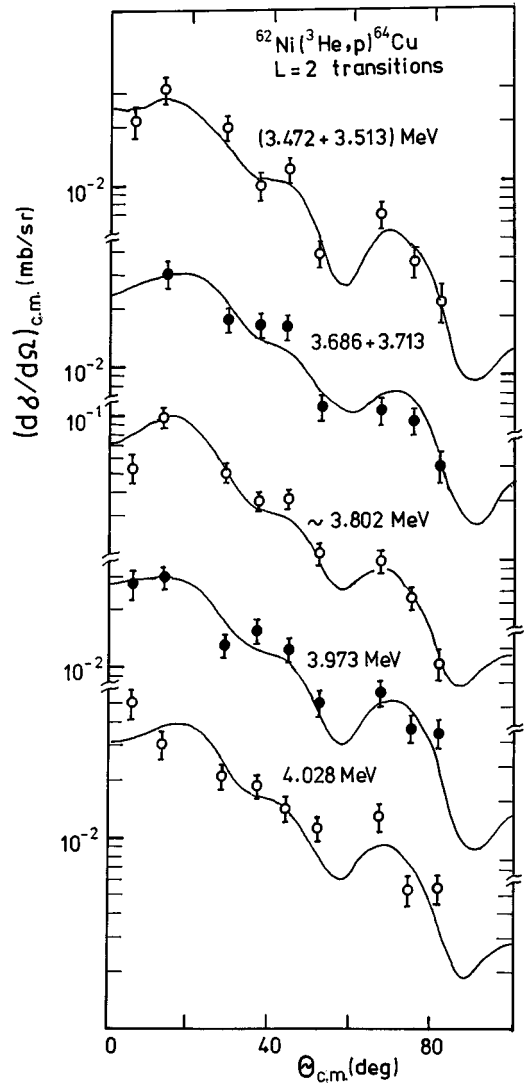


FIG. 11. Same as in Fig. 6.

Figs. 15 and 16, respectively. The first one needs both $L=2$ and 4 transfers while the data for the latter can be fitted with a purely $L=4$ transfer.

Figure 12 displays the DWBA predictions for $L=0$ transfers and to the angular distribution data for the 1.241, 1.299, 1.952, 2.455 MeV and the unresolved 2.801+2.827 MeV states, where the fits are reasonable. The angular distributions for the 1.509, 2.762, 3.397, 3.607, 3.902, and 4.137 MeV states have been reproduced well by the calculations with the $L=1$ transfer (Fig. 13). In Fig. 14 the $L=3$ DWBA predictions are compared to the data of the 2.990, 4.257, 5.043, 5.320 MeV states where the fits are certainly reasonable.

The angular distribution for the $(^3\text{He},p)$ reaction populating the 3.066 MeV state has been compared to the separate predictions with the $L=1$ and 3 transfers (Fig. 15), the latter being dominant at higher angles.

Figure 16 shows the angular distribution for the 1.602 and 3.302 MeV states which are well reproduced with the $L=4$ predictions assuming simple orbital configurations for the transferred pair. The angular distributions of the 4.316, 4.430, and 4.571 MeV states given in Fig. 17 have been fitted satisfactorily with the $L=5$ DWBA calculations.

V. DISCUSSION

Results on the levels of ^{64}Cu are summarized and compared to compiled results of previous works [32] in Table III. Newly assigned J^π values on the basis of the present work and those given in Ref. [32] are also displayed in the table. The states in ^{64}Cu at the 2.323, 3.231, 5.043, and 7.339 MeV excitations not found in the literature have been identified, the angular distributions measured and J^π limits deduced.

A. Normalization factor and shell-model amplitudes

The normalization factor N as defined in Eq. (1) has been deduced for several transitions to the low-lying shell model states [30], where the angular distributions are reproduced well by the DWBA predictions using the shell model spectroscopic amplitudes. The results are shown in Table IV. The N value deduced from the data of the ground analog state at the 6.821 MeV excitation, agrees favorably with the value $121 \times 10^4 \text{ MeV}^2 \text{ fm}^3$ as suggested in the write up of the CHUCK3 code [33]. Nevertheless, the N values from the different transitions vary over a range differing by an order of magnitude. Moreover the DWBA predictions for the ground

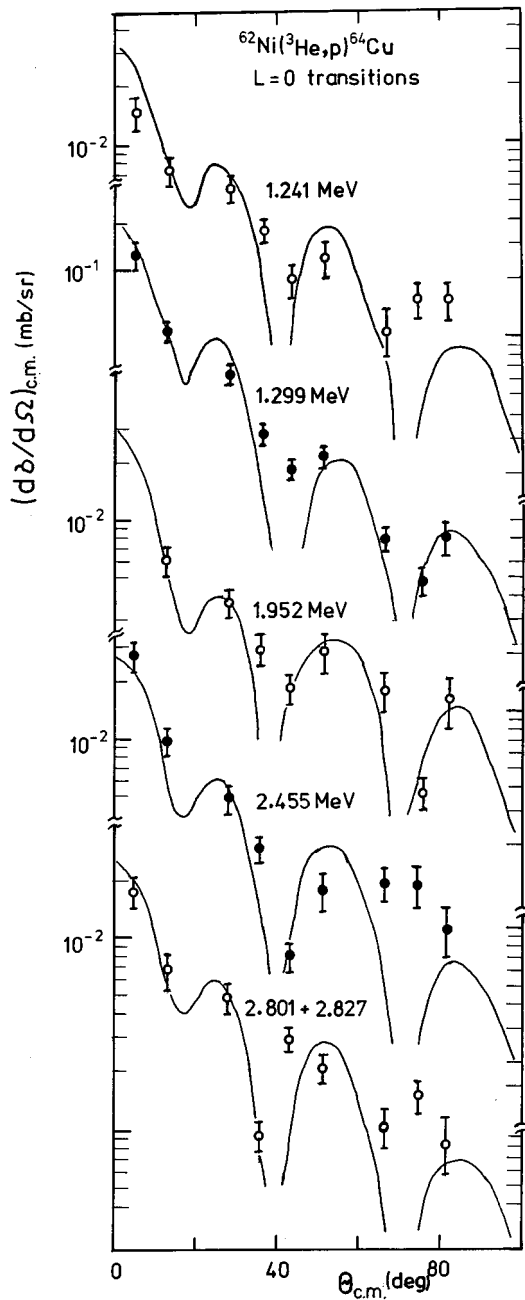


FIG. 12. The measured angular distributions are compared with $L=0$ DWBA predictions.

$(1^+;3)$ and 0.927 MeV $(1^+;3)$ transitions using the shell model spectroscopic amplitudes, are not close to the data for the former and far from the data for the latter (Fig. 4). The poor fits for the two transitions may be ascribed to (i) reaction processes other than the one-step transfer may not have a nonnegligible contribution to the reaction and/or (ii) the model space ($2p_{3/2}$, $1f_{5/2}$, and $2p_{1/2}$) in the shell model calculations may not be adequate even for the low-lying states in ^{64}Cu .

B. Spin-parity assignments

1. $L=0$ transitions

Six transitions with $L=0$ transfer (Fig. 12) have been identified. The $L=0$ assignment for the 2.455 MeV state

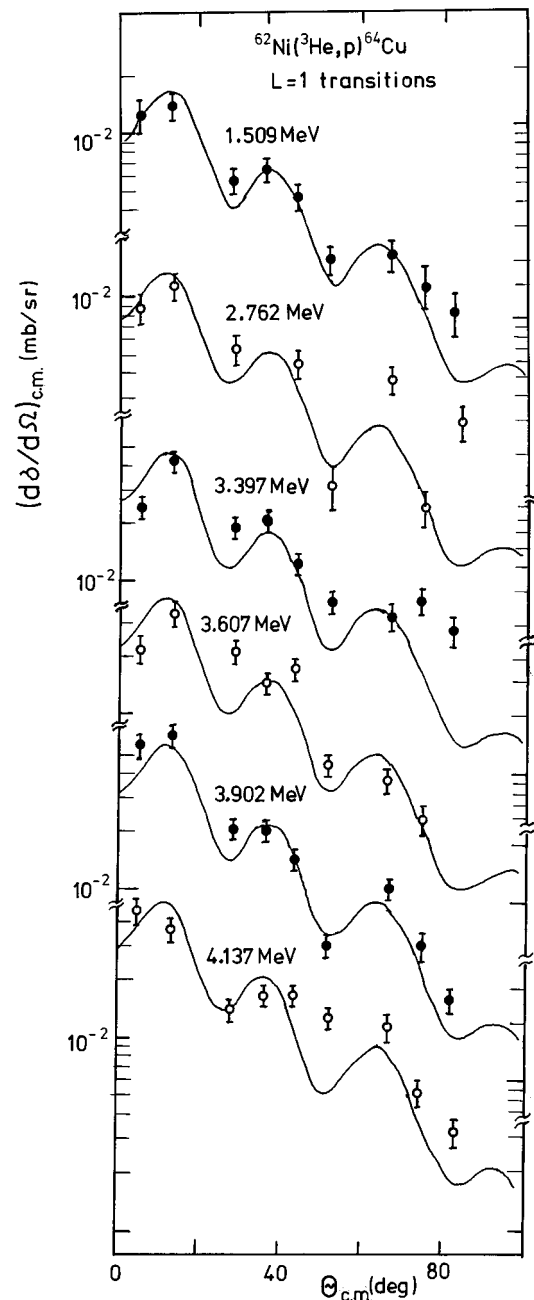


FIG. 13. The measured angular distributions are compared with $L=1$ DWBA predictions.

disagrees with the $L=1$ obtained in the (d,a) work [3], but conforms to the J^π assignment in Ref. [32]. In the unresolved $(2.801+2.827)$ MeV group, the latter state being stronger, $L=0$ can be attributed to the 2.827 MeV state. The present work in conjunction with the compiled work [12] would than assign $J^\pi=1^+$ to the 1.241 , 1.299 , 1.952 , 2.455 , and 2.827 MeV states.

2. $L=1$ transitions

Six transitions with $L=1$ transfer, shown in Fig. 13 have been observed. The present work supports the assignment of $J^\pi=2^-$ to the 1.509 MeV state; $J^\pi=(1^-,2^-)$ to the 2.762 and 3.902 MeV states and J^π limit $(0^- - 2^-)$ to the 3.397 , 3.607 , and 4.137 MeV states.

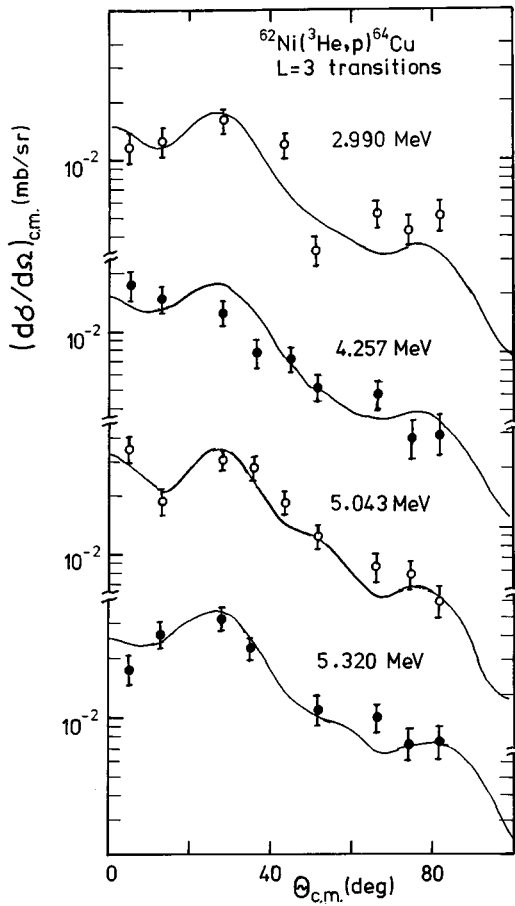


FIG. 14. The measured angular distributions are compared with $L=3$ DWBA predictions.

3. $L=2$ transitions

Thirty five $L=2$ transitions (Figs. 2, 6–11) have been observed up to $\sim E_x=8.2$ MeV. This is by far the largest number amongst all the L transitions studied in the present work. This may be ascribed to the fact that the angular momentum transfer $L=|k_i R_i - k_f R_f|$ (k and R being the wave number and the nuclear radius, respectively) at the nuclear surface for the reaction up to $\sim E_x=8.2$ MeV is in the limit (2–3).

The observed $L=2$ transfer in the present work does not conform to the compiled spin-parity [32] $J^\pi=0^+$ for the 0.878 MeV state, $(2^-, 3^-)$ for the 1.551 and 2.679 MeV states. There may be two separate states of opposite parities near to each of the latter two excitations. It is possible that the stronger of the composite group (1.741+1.775) MeV belong to $L=2$. The component states of the composite groups (3.472+3.513) MeV and (3.686+3.713) MeV have individually almost the same maximum $\sigma(\theta)$. Hence each of the 3.472, 3.513, 3.686, and 3.713 MeV states belongs to the $L=2$ transfer. The relative strengths for the component states of the composite group at (3.767+3.802) MeV could not be estimated as it presumably contains more than two states.

The present work confirms the spin-parity assignments $J^\pi=3^+$ to the 1.359 and 2.875 MeV states, 1^+ to the 1.440 and 1.689 MeV states, 2^+ to the 2.146 MeV states, makes a collective assignment with Ref. [32] of $J^\pi=3^+$ to the 1.853

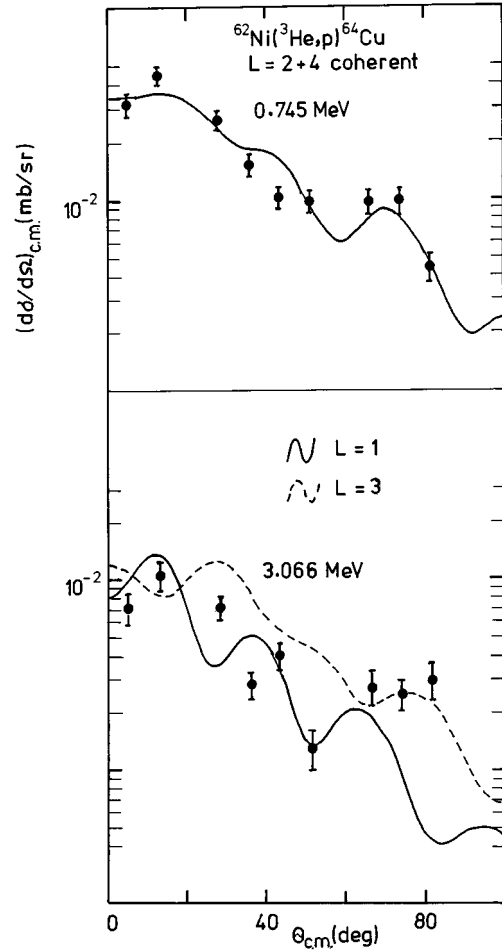


FIG. 15. The measured angular distributions are compared with the DWBA predictions. The solid curve in the top for the 0.745 MeV state is obtained using the shell model amplitudes in Table II. The solid curve from $L=1$ and the broken curve for $L=3$ in the bottom are the predictions for the 3.066 MeV state.

and 2.608 MeV states, and puts J^π limits ($1^+ - 2^+$) to the 3.265, 3.472, and 3.513 MeV states. The present work also confirms $J^\pi=2^+$ of the 8.188 MeV state and its status as the analog of the first 2^+ state of ^{64}Ni on the basis of the level position and J^π value. The assignment of J^π limits ($1^+ - 3^+$) to the 0.878, 1.320, 1.551, 1.741, 2.047, 2.092, 2.246, 2.290, 2.323, 2.369, 2.414, 2.515, 2.679, 2.718, 3.130, 3.189, 3.231, 3.686, 3.713, 3.973, and 4.028 MeV states and the dominant state of the group at the 3.802 MeV excitation follows naturally from the $L=2$ transfer observed for the associated transitions.

4. $L=0+2$ transitions

There are six transitions (Figs. 4 and 5) with $L=0+2$ transfers. Of these the ground, 0.663 MeV, and 0.927 MeV states have well-known [32] J^π . The present work confirms the $J^\pi=1^+$ for the 2.907 MeV state and assigns 1^+ to the 1.907 and 7.339 MeV states. It may be mentioned that the $J^\pi=1^+$ assignment to the 0.663 MeV level is from the studies of the $(p, n\gamma)$, (polarized n, γ), and (d, p) reactions and this J^π is adopted [32]. The $L=4$ transition in the $^{66}\text{Zn}(d, a)^{64}\text{Cu}$ reaction [3] to this level would mean that the

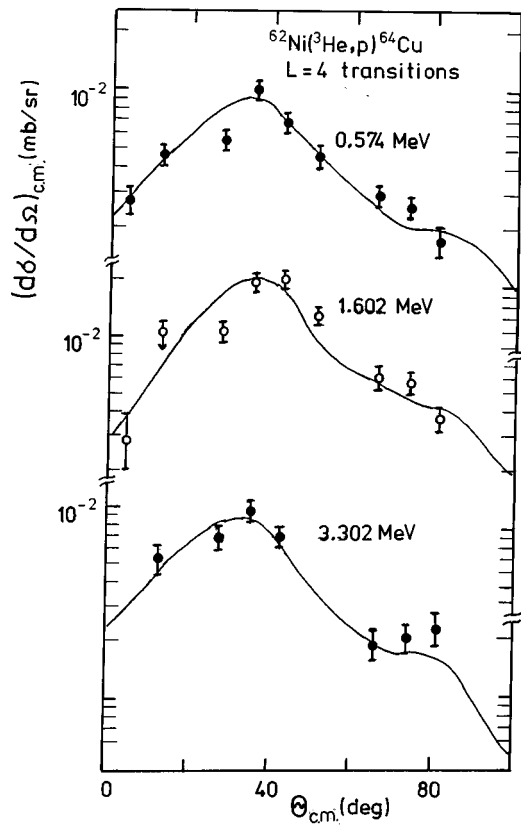


FIG. 16. The measured angular distributions are compared with $L=4$ DWBA predictions. The predictions for the 0.574 MeV state uses the shell model amplitudes in Table II.

level is a close doublet with $J^\pi=1^+$ for one of them. The other level, as seen in the (d,a) reaction, is then a good candidate for the missing $J^\pi=4_2^+$ shell model level (Fig. 3).

5. $L=3$ transitions

There are four transitions observed with $L=3$ transfer (Fig. 14). $L=3$ for the 4.257 MeV state disagrees with its spin-parity assignment $J^\pi=1^-,2^+$ from γ work [12]. The present work assigns $J^\pi=2^-$ to the 2.990 MeV using the results of the previous works [32] and makes a new assignment of the J^π limit as (2^--4^-) for the 5.043 and 5.320 MeV states.

6. $L=1+3$ transitions

There is one transition observed (Fig. 15) for the 3.066 MeV state, $L=1$ being dominant. The mixed L transfers suggest $J^\pi=2^-$ for the state.

7. $L=4$ transitions

There are three transitions observed with $L=4$ (Fig. 16). The DWBA prediction using the shell model amplitudes in Table II, gives a satisfactory fit to the data for the 0.574 MeV with $J^\pi=4^+$. The $L=4$ transfer observed for the 1.602 MeV state does not agree with $L=0+(2)$ from the (d,a) work [3]. The present work suggests the J^π limit as (3^+-5^+) for the 1.602 and 3.302 MeV states. As many as five levels are known to exist around $E_x \sim 1.60$ MeV with either parity having J values ranging over 1–6 [32]. The different L transfers

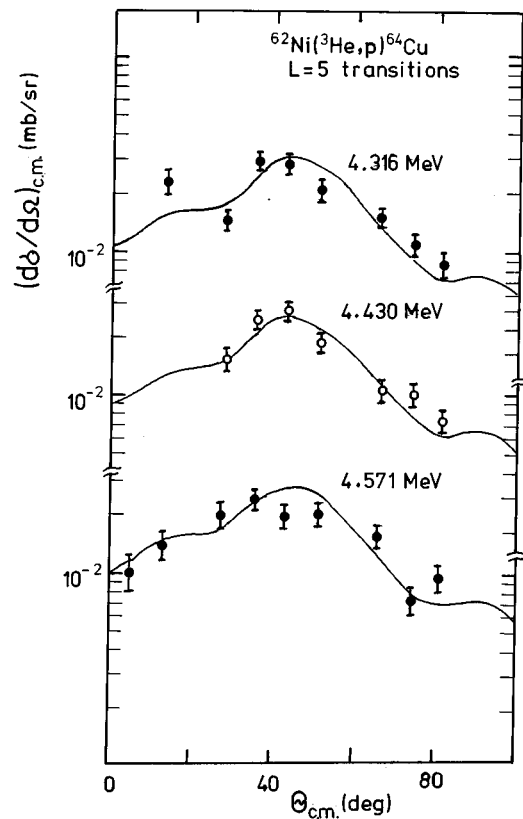


FIG. 17. The measured angular distributions are compared with $L=5$ DWBA predictions.

in the $(^3\text{He},p)$ reaction (present work) and (d,a) reaction [3] would therefore indicate the excitation of two different levels around $E_x \sim 1.60$ MeV.

8. $L=5$ transitions

Three transitions have been identified with the $L=5$ transfers (Fig. 17). The observed $L=5$ transfer does not agree with the compiled spin-parity assignments [32] $J^\pi=(1^+,2,3^-)$ for the 4.316 MeV state, $J^\pi=(1^-,2^-)$ for the 4.430 MeV state, and $J^\pi=9^+$ for the 4.571 MeV state. There may be states of opposite parities near to each of the three states. The present work makes a new assignment of the J^π limit (4^--6^-) for the three states, and further indicates clearly the nonexcitation of high spin negative parity states, known to exist at low excitation (below $E_x \sim 3$ MeV), through a single step process. The nonobservation of the 1.594 and 2.377 MeV levels with $J^\pi=6^-$ and 7^- , respectively, and found in the $^{62}\text{Ni}(a,pn\gamma)^{64}\text{Cu}$ reaction [14] are such examples. The configurations of the levels are suggested to be $[\pi p_{3/2}, \nu g_{9/2}]$ and $[\pi f_{5/2}, \nu g_{9/2}]$, respectively [14].

VI. CONCLUSION

DWBA calculations using the shell model spectroscopic amplitudes and with various sets of optical potential parameters have produced a bad fit to the data for the 0.927 MeV state and could not give a satisfactory fit to even the ground state data. Figure 4 shows the best possible fits amongst the

TABLE III. Summary on the levels of ^{64}Cu .

Gr. No.	Exct. energy (MeV)		$\sigma_{\text{cm}}(\theta)$ [$\mu\text{b/sr}$]		L transfer		J^π	
	a	b	c	d	a	f	b	e
00	0.000	0.000	40.4	26.0	0+2	0+(2)	1 ⁺	
01	0.160	0.159	14.2	5.3	2	2+(0)	2 ⁺	
02	0.278	0.278	6.2	2.7	2	2	2 ⁺	
03	0.362	0.362	16.4	7.8	2	4	3 ⁺	
04	0.574	0.575	10.0	4.5	4	4	(4) ⁺	4 ⁺
05	0.608	0.608	10.2	4.7	2	2	2 ⁺	
06	0.663	0.663	4.6	2.1	0+2	4	1 ⁺	
		0.739					2 ⁺	3 ⁺
07	0.745	0.746	45.0	17.7	2+4	2+(4)	3 ⁺	
08	0.878	0.878	4.9	3.0	2		(0) ⁺	(1 ⁺ -3 ⁺)
09	0.927	0.927	106.5	30.3	0+2	0+(2)	(1) ⁺	
10	1.241	1.241	14.6	4.4	0	0+(2)	1 ⁽⁺⁾ ,2 ⁽⁺⁾	1 ⁺
		1.243					(≤ 3)	
11	1.299	1.298	120.4	26.2	0	0+2	(1 ⁺)	1 ⁺
12	1.320	1.320	21.5	7.8	2		(0-2)	1 ⁺ ,2 ⁺
13	1.359	1.354	8.6	4.4	2	4+(2)	(3 ⁺)	3 ⁺
14	1.440	1.438	18.4	7.8	2	0+(2)	(1) ⁺	1 ⁺
15	1.509	1.499	13.6	5.3	1	(1+3)	2 ⁻	2 ⁻
16	1.551	1.551	37.3	14.8	2	2	(2 ⁻ ,3 ⁻)	(1 ⁺ -3 ⁺)
17	1.602	1.607	19.0	9.7	4	0+(2)	(2 ⁺ ,3,4 ⁻)	(3 ⁺ -5 ⁺)
18	1.689	1.683	213.0	91.9	2	0+2	(≤ 3)	1 ⁺
19	1.741	1.739	32.4				(3 ⁺ -5 ⁺)	(1 ⁺ -3 ⁺)
		1.742		16.6	2		(1 ⁺ -3 ⁺)	
20	1.775	1.769	9.5				(3-5) ⁺	(1 ⁺ -3 ⁺)
		1.779					1 ⁺ ,2 ⁺	
21	1.853	1.852	9.5	3.3	2	4	(1 ⁺ ,2 ⁺)	3 ⁺
22	1.907	1.905	47.3	11.0	2+(0)	(0+2)	(1 ⁺ ,2)	1 ⁺
23	1.952	1.940	6.1	2.1	0	2+(0)	(1-3) ⁺	1 ⁺
24	2.047	2.042	27.3	11.3	2	4+(2)	(≤ 3)	(1 ⁺ -3 ⁺)
		2.050					1 ⁺ ,2,3	
		2.053					(≤ 4)	
25	2.092	2.092	10.4	6.0	2	2+(0)	(1-3) ⁺	(1 ⁺ -3 ⁺)
26	2.146	2.145	5.2	1.9	2	4+(2)	(2 ⁺)	2 ⁺
27	2.246	2.244	20.0	8.7	2	(2)	(≤ 3)	(1 ⁺ -3 ⁺)
		2.251					(4,5,6)	
28	2.290	2.301	29.6	12.6	2	2	(≤ 3)	(1 ⁺ -3 ⁺)
29	2.323 ^g	2.323	36.5	12.5	2			(1 ⁺ -3 ⁺)
30	2.369	2.360	9.4	3.7	2		(≤ 3)	(1 ⁺ -3 ⁺)
		2.376					(1 ⁺)	
		2.378					(7 ⁻)	
		2.381					(≤ 3)	
31	2.414	2.417	8.4	3.4	2		(≤ 3)	(1 ⁺ -3 ⁺)
32	2.455	2.457	26.5	6.2	0	(1)	(1 ⁺ ,2,3 ⁺)	1 ⁺
33	2.515	2.507	42.0	12.5	2		(≤ 3)	(1 ⁺ -3 ⁺)
		2.522						
34	2.608	2.607	16.0	6.5	2	4		3 ⁺
35	2.679	2.670	22.1	9.2	2	(3)+1	(1 ⁻ ,2 ⁻)	(1 ⁺ -3 ⁺)
36	2.718	2.726	14.4	6.0	2	2	(1 ⁺ ,2,3 ⁺)	(1 ⁺ -3 ⁺)
37	2.762	2.757	11.5	4.6	1		(1 ⁻ ,2 ⁻);(3 ⁺)	1 ⁻ ,2 ⁻
38	2.801	2.807	8.5				(1 ⁻ ,2 ⁻)	
				4.3	0			
39	2.827	2.830	10.6			(0+2)	(≤ 3)	1 ⁺
40	2.875	2.869	15.7	7.0	2	4	(3 ⁺)	3 ⁺

TABLE III. (Continued).

Gr. No.	Exct. energy (MeV)		$\sigma_{\text{cm}}(\theta)$ [$\mu\text{b/sr}$]		L transfer		J^π	
	a	b	c	d	a	f	b	e
41	2.907	2.896	16.7	5.4	(0+2)	(0+2)	(1 ⁺)	1 ⁺
42	2.990	2.985	15.1	8.6	3		(1 ⁻ , 2 ⁻)	2 ⁻
		3.013					(1 ⁻ , 2 ⁻)	
43	3.066	3.051	10.0	5.0	1+(3)		(≤ 3)	2 ⁻
		3.072					(2 ⁻ -4 ⁻)	
44	3.130	3.126	28.2	10.4	2		(≤ 3)	(1 ⁺ -3 ⁺)
45	3.189	3.190	23.9	9.4	2		8 ⁻	(1 ⁺ -3 ⁺)
		3.191					(≤ 4)	
		3.207					(0,1,2)	
46	3.231 ^g		20.0	5.5	2			(1 ⁺ -3 ⁺)
47	3.265	3.258	9.7	4.7	2		(0,1,2)	(1 ⁺ , 2 ⁺)
48	3.302	3.290	9.2	4.8	4			(3 ⁺ -5 ⁺)
		3.313					(0,1,2)	
49	3.397	3.412	41.2	15.9	1		≤ 3	(0 ⁻ -2 ⁻)
50	3.472	3.475	16.4		2		(0,1,2)	(1 ⁺ , 2 ⁺)
				11.3				
51	3.513	3.511	13.7				(1,2)	(1 ⁺ , 2 ⁺)
52	3.607	3.603	25.7	12.2	1		(≤ 3)	(0 ⁻ -2 ⁻)
53	3.686	3.687	12.3		2			(1 ⁺ -3 ⁺)
				12.4			(≤ 3)	
54	3.713	3.712	17.7					(1 ⁺ -3 ⁺)
55	3.767	3.763						
			97.0	34.7	2			(1 ⁺ -3 ⁺)
56	3.802	3.799					(9 ⁺)	
		3.803					(≤ 3)	
57	3.902	3.900	60.3	21.4	1		(1 ⁻ , 2 ⁻)	(1 ⁻ , 2 ⁻)
58	3.973	3.987	29.5	13.0	2			(1 ⁺ -3 ⁺)
59	4.028	4.034	51.8	18.5	2		(0,1,2)	(1 ⁺ -3 ⁺)
60	4.137	4.141	45.4	17.3	1		(0 ⁻ -2 ⁻)	(0 ⁻ -2 ⁻)
61	4.257	4.264	17.1	8.5	3		(1,2 ⁺)	(2 ⁻ -4 ⁻)
62	4.316	4.328	29.0	15.1	5		(1,2 ⁺)	(4 ⁻ -6 ⁻)
63	4.430	4.433	27.0	15.9	5		(1 ⁻ , 2 ⁻)	(4 ⁻ , 6 ⁻)
		4.444					(≤ 3)	
64	4.571	4.570	24.0	17.5	5		(9 ⁺)	(4 ⁻ -6 ⁻)
65	5.043 ^g		35.0	18.4	3			(2 ⁻ -4 ⁻)
66	5.320	5.320	32.0	16.5	3			(2 ⁻ -4 ⁻)
		6.810					(0 ⁺)	
67	6.821	6.826	483.3	131.6	0		(0 ⁺)	0 ⁺
68	7.339 ^g		28.0	8.7	0+(2)			1 ⁺
69	8.188	8.170	281.9	115.5	2		(2 ⁺)	2 ⁺

^aPresent work.^bNuclear data [32].^cMaximum cross section.^dAverage 5°-80°.^eNew assignment of J^π .^f(d, a) reaction [3].^gNew level.

various possible choices of the optical model potentials. However, the fits greatly improve with a modified set of spectroscopic amplitudes. Moreover, the normalization factors deduced from the transitions with satisfactory fits have a

spread of an order of magnitude. This suggests that the shell model calculations in the model space ($2p_{3/2}$, $1f_{5/2}$, and $2p_{1/2}$) may not be adequate for generating the wave functions for the states in ^{62}Ni and ^{64}Cu . Another possibility is

TABLE IV. Normalization factors for different transitions.

E_x (MeV)	$J^\pi; T$	ΔT	$\sigma_{\text{exp}}/\sigma_{DW}$	$N=N D_{01} ^2/2$ ($\text{MeV}^2 \text{fm}^3$) $\times 10^4$
0.160	$2^+; 3$	0+1	1.87 ± 0.29	226.3 ± 35.1
0.278	$2^+; 3$	0+1	0.17 ± 0.02	20.6 ± 2.4
0.362	$3^+; 3$	0	2.73 ± 0.80	275.3 ± 80.7
0.574	$4^+; 3$	0+1	0.27 ± 0.03	32.7 ± 3.6
0.608	$2^+; 3$	0+1	0.22 ± 0.03	26.6 ± 3.6
6.821	$0^+; 4$	1	0.94 ± 0.03	113.7 ± 3.6

the involvement of reaction processes other than the direct transfer, present in the reaction. One may verify this by investigating the contributions from various two-step and sequential processes for a transition with simplest configuration viz. the ground analog transition.

The present work confirms the J^π values of several levels and in conjunction with the compiled work [32] has made unique spin-parity assignments to several levels as well as trimmed down the J^π limits of many of the levels of ^{64}Cu . There are discrepancies found for the 1.551, 2.679, 4.257,

and 4.571 MeV states where the observed L transfers do not conform to the compiled J^π values in Ref. [32]. This may be ascribed, in some cases at least, to different states with excitation energies very close to the above mentioned levels. In an odd-odd nucleus such as ^{64}Cu , where the level densities are expected to be high, this is not an impossible proposition. Different close-lying levels may be selectively populated in different reactions.

ACKNOWLEDGMENTS

The authors are indebted to Dr. D. L. Watson of the University of York for kindly sending us the exposed emulsion plates from the University of Bradford. They are also thankful to Professor P. D. Kunz of the University of Colorado for sending us DWUCK4 and CHUCK3 codes and to Dr. J. D. Brown and Dr. Z. Q. Mao of Princeton University for sending us the shell model spectroscopic amplitudes. The financial support and hospitality of the International Center for Theoretical Physics (ICTP) accorded to one of us (A.K.B.) is gratefully acknowledged. He would also like to thank the Swedish Agency for Research Cooperation with Developing Countries (SAREC) for financial support during his visit to the ICTP.

-
- [1] C.C. Lu, M.S. Zisman, and B.G. Harvey, Phys. Rev. **186**, B1086 (1969).
- [2] R.P. de Figueiredo, M. Mazar, and W.W. Buechner, Phys. Rev. **186**, 873 (1969).
- [3] Y.S. Park and W.W. Daehnick, Phys. Rev. **180**, 1082 (1969).
- [4] B.Ya. Guzhoskii, S.N. Abramovich, A.G. Zvenigorodskii, and S.V. Trusillo, Sov. J. Nucl. Phys. **16**, 123 (1973).
- [5] J. Bleck, R. Butt, K.H. Lindenberger, W. Ribbe, and W. Zeitz, Nucl. Phys. **A197**, 620 (1972).
- [6] W.T. Bass and P.H. Stelson, Phys. Rev. C **2**, 2154 (1970).
- [7] J.D. Sherman, E.R. Flynn, Ole Hansen, N. Stein, and J.W. Sunier, Phys. Lett. **67B**, 275 (1977).
- [8] K. Maeda, H. Orihara, T. Murakami, S. Nishihara, T. Nakagawa, K. Miura, and H. Ohnuma, Nucl. Phys. **A403**, 1 (1983).
- [9] P.W. Green and D.M. Sheppard, Nucl. Phys. **A274**, 125 (1976).
- [10] E.B. Shera and H.H. Bolotin, Phys. Rev. **169**, 940 (1968).
- [11] J. Kopecky, F. Stecher-Rasmussen, and K. Abraham, Nucl. Phys. **A215**, 54 (1973).
- [12] M.G. Delfini, J. Kopecky, J.B.M. De Haas, H.I. Liou, R.E. Chrien, and P.M. Endt, Nucl. Phys. **A410**, 513 (1983).
- [13] S.J. Hjorth and L.H. Allen, Ark. Fys. **33**, 207 (1967).
- [14] T.U. Chan, M. Agard, J.F. Bruandet, A. Giorni, and J.P. Longeque, Nucl. Phys. **A257**, 413 (1976).
- [15] H.J. Young and J. Rapaport, Bull. Am. Phys. Soc. **13**, 105 (1968).
- [16] P.D. Kunz (private communication).
- [17] H.J. Trost, P. Lezoch, and V. Srohbusch, Nucl. Phys. **A462**, 333 (1987).
- [18] J.R. Shepard, W.R. Zimmerman, and J.J. Kraushaav, Nucl. Phys. **A275**, 189 (1977).
- [19] J.J.H. Menet, E.E. Gross, J.J. Malanify, and A. Zucker, Phys. Rev. C **4**, 1114 (1971).
- [20] F.D. Becchetti and G.W. Greenlees, Phys. Rev. **182**, 1190 (1969).
- [21] F.G. Perey, Phys. Rev. **131**, 745 (1963).
- [22] B.A. Watson, P.P. Singh, and R.E. Segel, Phys. Rev. **182**, B977 (1969).
- [23] H.M. Sen Gupta, J.B.A. England, F. Khazaie, E.M.E. Rawas, and G.T.A. Squire, Nucl. Phys. **A517**, 82 (1990); M.A. Basher, H.R. Siddiqui, A. Husain, A.K. Basak, and H.M. Sen Gupta, Phys. Rev. C **45**, 1575 (1992).
- [24] F.G. Perey, *Proceedings of the Conference on Direct Interactions and Nuclear Reaction Mechanisms* (Gordon and Breach, New York, 1963), p. 125.
- [25] N.K. Glendenning, *Nuclear Spectroscopy and Reactions* (Academic, New York, 1975), Pt. D, p. 319.
- [26] R.H. Bassel, Phys. Rev. **149**, 791 (1966).
- [27] I.S. Towner and J.C. Hardy, Adv. Phys. **18**, 401 (1969).
- [28] J.C. Hardy and I.S. Towner, Phys. Lett. **25B**, 98 (1967).
- [29] H. Nann, B. Hubert, and R. Bass, Nucl. Phys. **A176**, 553 (1971).
- [30] J. D. Brown and Z. Q. Mao (private communication).
- [31] J.E. Koops and P.W.M. Glaudemans, Z. Phys. A **280**, 181 (1977); (private communication).
- [32] B. Singh, Nucl. Data Sheets **62**, 603 (1991).
- [33] P.D. Kunz (private communication).